

000 DYNAMIC PREFERENCE CALIBRATION: META- 001 002 LEARNING SOFT LABELS FOR ROBUST ALIGNMENT 003 004

005 **Anonymous authors**

006 Paper under double-blind review

007 008 ABSTRACT 009

011 Noise in preference data significantly impedes the robust alignment of large lan-
012 guage models (LLMs) with human values. Existing methods that rely on global
013 noise assumptions or static pre-processing heuristics are often insufficient, as they
014 fail to address the instance-specific and dynamic nature of preference noise. To
015 overcome these limitations, we introduce Dynamic Preference Calibration, a novel
016 framework that meta-learns to generate adaptive soft labels directly from noisy
017 data. Our approach employs a lightweight meta-learner that maps a perplexity dif-
018 ference (PPLDiff) signal to a calibrated soft label. Crucially, the power of our dy-
019 namic approach stems from calculating this PPLDiff signal online, using the main,
020 evolving LLM itself. This creates a symbiotic loop where the main model’s im-
021 proving understanding continuously informs and refines the calibration strategy,
022 allowing it to co-evolve. Guided by a small, clean meta-dataset, the meta-learner
023 is optimized to produce labels that maximize alignment performance. Extensive
024 experiments on benchmark datasets demonstrate that our method establishes a new
025 state-of-the-art for noisy preference alignment, significantly outperforming strong
026 baselines. It maintains high performance and stability even under extreme noise
027 levels up to 40% label flips, highlighting the promise of meta-learning for building
028 fundamentally more robust and reliable alignment techniques.

029 1 INTRODUCTION 030

031 Large Language Models (LLMs) have demonstrated remarkable capabilities across a vast range of
032 natural language tasks Brown et al. (2020); Anil et al. (2023); Touvron et al. (2023). Aligning
033 these models with human values to ensure they are helpful, honest, and harmless is a critical pre-
034 requisite for their safe deployment Lee et al. (2023); Askell et al. (2021); Amodei et al. (2016).
035 Learning from human preferences, particularly through methods like Direct Preference Optimiza-
036 tion (DPO) Rafailov et al. (2023), has emerged as a powerful and prominent alignment paradigm.
037 However, the efficacy of this paradigm is critically dependent on the quality of the preference data,
038 which is often compromised by noise from sources such as annotator subjectivity, task misinterpre-
039 tation, or imperfections in AI-generated feedback Bai et al. (2022b); Liang et al. (2024); Ziegler
040 et al. (2019). Such noise can severely undermine the alignment process, leading to models that fail
041 to capture true human intent.

042 Existing approaches to mitigate preference noise are fundamentally limited by their reliance on
043 static assumptions and offline corrections. First, robust loss-based methods like Conservative DPO
044 (cDPO) Mitchell (2023) and Robust DPO (rDPO) Chowdhury et al. (2024) typically rely on a *global*
045 *noise ratio* estimated from a clean validation set. This “one-size-fits-all” correction lacks instance-
046 level granularity and fails to account for the fact that noise is not uniformly distributed across the
047 data. Second, data-centric methods such as Perplexity-aware Correction (PerpCorrect) Kong et al.
048 (2024) attempt to identify and correct noisy pairs using signals like perplexity differences (PPLDiff).
049 While promising, these methods are fundamentally limited by their reliance on *static, heuristic-
050 based rules* applied during pre-processing. They typically compute PPLDiff from a fixed surrogate
051 model, providing only a static snapshot of preference consistency. This correction logic cannot adapt
052 or improve, even as the main LLM being aligned becomes more capable and its own understanding
053 of the preferences evolves. This reveals a critical gap: the need for a robust alignment mechanism
054 that can learn to correct noise at an instance-specific level and dynamically adapt its strategy in
055 lockstep with the language model’s own learning process.

To address this gap, we propose a new paradigm for robust alignment: Dynamic Preference Calibration. We introduce Meta Soft Preference Optimization (MSPO), a novel framework that instantiates this paradigm. As illustrated in Figure 1, MSPO employs a meta-learner not merely to filter noise, but to **calibrate** the original preference signals, dynamically generating optimized soft labels that represent a more accurate preference strength. Instead of relying on static rules, MSPO learns an adaptive function that maps a noise-indicative signal to a **calibrated preference strength**. Crucially, the primary input to this function—the perplexity difference (PPLDiff)—is calculated using the current main LLM $\pi_{\theta(t)}$ at each step of training. This creates a powerful symbiotic relationship where the main model’s evolving understanding continuously informs and improves the noise calibration strategy.

Through extensive experiments, we demonstrate that MSPO establishes a new state-of-the-art in robust LLM alignment. Our method significantly outperforms strong baselines, including those based on global noise ratios and static perplexity-based corrections, especially under high-noise conditions. The results validate the effectiveness of our meta-learning approach and highlight the substantial benefits of leveraging dynamic, model-intrinsic signals for online noise correction.

2 PRELIMINARIES

This section reviews the foundational concepts upon which our work is built: Direct Preference Optimization (DPO), its extension to handle soft preferences (GDPO), and the use of perplexity difference as a signal for preference consistency.

2.1 DIRECT PREFERENCE OPTIMIZATION (DPO)

Direct Preference Optimization (DPO) Rafailov et al. (2023) offers an elegant and effective method for aligning Large Language Models (LLMs) with human preferences, bypassing the complexities of traditional reinforcement learning from human feedback (RLHF). Given a preference dataset $\mathcal{D} = \{(x^{(i)}, y_w^{(i)}, y_l^{(i)})\}$, where for each prompt x , y_w is the preferred response and y_l is the dispreferred response, DPO directly optimizes the language model policy π_θ . It does so by maximizing the likelihood of the observed preferences under a Bradley-Terry model.

The core of the DPO objective is to increase the relative log-probability of the preferred response over the dispreferred one, compared to a fixed reference policy π_{ref} . This relationship is captured by the log-ratio term, defined as:

$$h_{\pi_\theta}(x, y_w, y_l) = \log \frac{\pi_\theta(y_w | x)}{\pi_{ref}(y_w | x)} - \log \frac{\pi_\theta(y_l | x)}{\pi_{ref}(y_l | x)}. \quad (1)$$

The DPO loss is then formulated as the negative log-likelihood of the preferences, encouraging h_{π_θ} to be positive:

$$\mathcal{L}_{DPO}(\pi_\theta; \pi_{ref}) = -\mathbb{E}_{(x, y_w, y_l) \sim \mathcal{D}} [\log \sigma(\beta \cdot h_{\pi_\theta}(x, y_w, y_l))], \quad (2)$$

where σ is the sigmoid function and β is a temperature parameter that controls the strength of the preference modeling.

2.2 GEOMETRIC-AVERAGED DPO (GDPO) WITH SOFT LABELS

Human preferences are often not binary; they come with varying degrees of strength and certainty. To capture this nuance, Geometric-averaged DPO (GDPO) Furuta et al. (2024) extends the DPO

108 framework to incorporate soft preference labels. A soft label $\hat{p} \in [0.5, 1.0]$ is introduced to represent
 109 the estimated probability that y_w is truly preferred over y_l , i.e., $P(y_w \succ y_l | x)$.
 110

111 GDPO then modulates the core log-ratio term (Eq. 1) by a scaling factor derived from this soft label,
 112 $(2\hat{p} - 1)$. This factor ranges from 0 (for $\hat{p} = 0.5$, complete uncertainty) to 1 (for $\hat{p} = 1.0$, full
 113 confidence). The resulting loss function is:

$$\mathcal{L}_{\text{GDPO}}(\pi_\theta; \pi_{\text{ref}}, \hat{p}) = -\mathbb{E}_{(x, y_w, y_l, \hat{p}) \sim \mathcal{D}} [\log \sigma(\beta(2\hat{p} - 1)h_{\pi_\theta}(x, y_w, y_l))]. \quad (3)$$

114 This formulation allows for a more fine-grained alignment process. However, its success is critically
 115 dependent on the availability of reliable and well-calibrated soft labels \hat{p} , a major challenge in the
 116 presence of noisy data.
 117

119 2.3 PERPLEXITY DIFFERENCE AS A NOISE INDICATOR

120 The perplexity (PPL) of a text sequence under a language model π_θ is a measure of how well the
 121 model predicts that sequence. The difference in log-perplexity between two responses, y_w and y_l ,
 122 given a prompt x , can serve as a powerful signal for preference consistency and potential noise Kong
 123 et al. (2024). This Perplexity Difference (PPLDiff) is defined as:
 124

$$\text{PPLDiff}(x, y_w, y_l; \pi_\theta) = \log \text{PPL}([x; y_w]; \pi_\theta) - \log \text{PPL}([x; y_l]; \pi_\theta), \quad (4)$$

125 where $[x; y]$ denotes the concatenation of the prompt and the response. A negative PPLDiff suggests
 126 that π_θ finds the nominally preferred response y_w more plausible (i.e., less perplexing) than y_l ,
 127 aligning with the given preference label. Conversely, a large positive PPLDiff indicates a conflict
 128 between the model’s understanding and the label, signaling a potential mislabeling. This quantifiable
 129 signal forms the basis for our meta-learner’s input in MSPO.
 130

132 3 METHODOLOGY

133 Building on the preliminaries, this section introduces our proposed framework, Meta Soft Preference
 134 Optimization (MSPO). We first present the overall framework, detailing its core components
 135 and design philosophy. We then describe the bilevel optimization procedure that enables the joint
 136 training of the main language model and the meta-learner.
 137

140 3.1 THE MSPO FRAMEWORK

141 The core idea of our Dynamic Preference Calibration paradigm is to reframe robust alignment as a
 142 meta-learning task, which our MSPO framework achieves through a dedicated meta-learner. Instead
 143 of using noisy preference labels directly, MSPO learns a dedicated meta-learner, $V(\cdot; \phi)$, to dynam-
 144 ically generate a well-calibrated soft preference label \hat{p}_ϕ for each training instance. This allows for
 145 fine-grained, instance-specific noise correction. The overall architecture is depicted in Figure 2.
 146

147 3.1.1 ADAPTIVE LABEL GENERATION VIA META-LEARNING

148 The central component of MSPO is the meta-learner $V(\cdot; \phi)$, a lightweight neural network par-
 149 meterized by ϕ . Its purpose is to learn an adaptive function that maps a noise-indicative signal to a
 150 **calibrated** soft preference label $\hat{p}_\phi \in [0, 1]$. This generated label \hat{p}_ϕ is then used within a GDPO-
 151 style loss (Eq. 3) to guide the optimization of the main LLM policy, π_θ . By learning this mapping,
 152 MSPO moves beyond fixed heuristics, allowing the noise-correction strategy itself to be optimized
 153 for the downstream alignment task.
 154

155 3.1.2 DYNAMIC PERPLEXITY DIFFERENCE AS THE INPUT SIGNAL

156 The choice of input signal for the meta-learner is critical. The choice of input signal is critical and
 157 represents the cornerstone of our dynamic approach: we utilize a Perplexity Difference (PPLDiff)
 158 signal that is computed online using the current main policy. For each training sample (x, y_1, y_2) at
 159 step t , the PPLDiff is computed using the **current main policy** $\pi_{\theta(t)}$:
 160

$$\text{PPLDiff}^{(t)} = \text{PPLDiff}(x, y_1, y_2; \pi_{\theta(t)}). \quad (5)$$

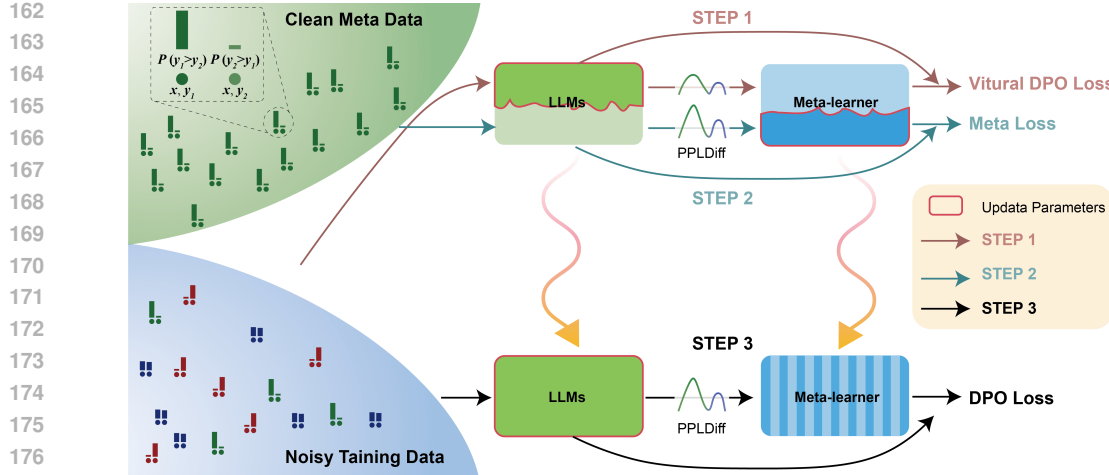


Figure 2: Overview of the MSPO framework. A meta-learner $V(\cdot; \phi)$ processes PPLDiff, calculated using the current main LLM $\pi_{\theta(t)}$, to generate optimized soft labels \hat{p}_ϕ . These labels guide the training of π_θ via a GDPO-style preference loss. V is optimized using a clean meta-dataset D_{meta} to enhance π_θ 's alignment performance.

This online computation ensures that the meta-learner receives a signal that reflects the LLM's most up-to-date understanding, creating a symbiotic loop where the model's progress informs its own robust training. The meta-learner then produces the soft label as:

$$\hat{p}_\phi = V(\text{PPLDiff}^{(t)}; \phi). \quad (6)$$

3.2 BILEVEL OPTIMIZATION OF MSPO

The parameters of the main LLM, θ , and the meta-learner, ϕ , are optimized jointly through a bilevel process. This process allows the meta-learner to receive feedback on the quality of its generated labels based on their downstream impact on the main LLM's performance on clean data. At each training iteration t , the optimization unfolds in three key steps:

STEP 1: Compute Virtual LLM Parameter Update. The first step simulates how the main LLM would be updated using the soft labels generated by the *current* meta-learner $V(\cdot; \phi^{(t)})$. For a mini-batch \mathcal{B}_{train} from the noisy training set, we compute a virtual main loss, $\mathcal{L}_{main}^{virtual}$:

$$\mathcal{L}_{main}^{virtual}(\theta; \phi^{(t)}) = -\frac{1}{|\mathcal{B}_{train}|} \sum_{\mathcal{B}_{train}} \log \sigma(\beta(2\hat{p}_{\phi^{(t)}} - 1)h_{\pi_\theta}(x, y_1, y_2)). \quad (7)$$

A one-step gradient descent on this loss yields the virtual LLM parameters, $\theta_{virtual}(\phi^{(t)})$, representing a hypothetical “lookahead” state:

$$\theta_{virtual}(\phi^{(t)}) = \theta^{(t)} - \alpha \nabla_\theta \mathcal{L}_{main}^{virtual}(\theta; \phi^{(t)})|_{\theta=\theta^{(t)}}. \quad (8)$$

STEP 2: Update Meta-learner Parameters. Next, we evaluate the quality of this virtual update on a mini-batch \mathcal{B}_{meta} from the clean meta-dataset D_{meta} . The meta-loss, \mathcal{L}_{meta} , is the standard DPO loss of the virtual LLM on this clean data:

$$\mathcal{L}_{meta}(\phi^{(t)}) = \mathbb{E}_{(x_m, y_{wm}, y_{lm}) \sim \mathcal{B}_{meta}} [\mathcal{L}_{DPO}(\pi_{\theta_{virtual}(\phi^{(t)})}; \pi_{ref})]. \quad (9)$$

This loss quantifies how well $V(\cdot; \phi^{(t)})$ guides the LLM towards trusted preferences. The meta-learner's parameters are then updated by descending this meta-loss:

$$\phi^{(t+1)} = \phi^{(t)} - \eta_{meta} \nabla_\phi \mathcal{L}_{meta}(\phi^{(t)}). \quad (10)$$

STEP 3: Update Main LLM Parameters. Finally, the actual parameters of the main LLM, $\theta^{(t)}$, are updated. This update uses the *newly improved* meta-learner, $V(\cdot; \phi^{(t+1)})$. A fresh set of soft

216 labels, $\hat{p}_{\phi^{(t+1)}}$, are generated for the original batch \mathcal{B}_{train} . The main LLM’s loss is calculated with
 217 these refined labels:

$$219 \quad \mathcal{L}_{main}(\theta; \phi^{(t+1)}) = -\frac{1}{|\mathcal{B}_{train}|} \sum_{\mathcal{B}_{train}} \log \sigma(\beta(2\hat{p}_{\phi^{(t+1)}} - 1)h_{\pi_\theta}(x, y_1, y_2)). \quad (11)$$

221 The main LLM parameters are then updated via a standard gradient step on this loss:
 222

$$223 \quad \theta^{(t+1)} = \theta^{(t)} - \alpha \nabla_{\theta} \mathcal{L}_{main}(\theta; \phi^{(t+1)})|_{\theta=\theta^{(t)}}. \quad (12)$$

225 This three-step cycle allows the meta-learner and the main LLM to co-evolve, continuously adapting
 226 the noise-correction strategy. The complete procedure is detailed in Algorithm 1 in Appendix A.
 227

228 **Theoretical Justification.** The bilevel optimization process of MSPO is not merely an empirical
 229 heuristic. From a theoretical standpoint, it can be interpreted as learning an implicit weighting
 230 scheme for noisy preferences. Furthermore, as we detail in Appendix B, the performance of the
 231 learned meta-policy is backed by a generalization bound, which connects its effectiveness to the
 232 size of the clean meta-dataset and the complexity of the meta-learner. This provides a theoretical
 233 grounding for our data-driven approach.

235 4 EXPERIMENTS

237 We conduct a comprehensive set of experiments to validate the effectiveness of our Dynamic Pref-
 238 erence Calibration paradigm, as instantiated by MSPO, and to analyze its underlying mechanisms.
 239 We aim to answer key questions regarding its robustness, the contribution of its core components,
 240 its internal behavior, and its training dynamics.

242 4.1 EXPERIMENTAL SETUP

244 **Core Configuration.** Our evaluation is performed on two standard preference benchmarks:
 245 Golden HH Bai et al. (2022a) and OASST1 Köpf et al. (2023). We inject random label flipping
 246 noise into the training sets at rates from 0% to 40%. The base models for all alignment methods are
 247 Supervised Fine-Tuned (SFT) versions of Llama-2-7B Touvron et al. (2023) and Phi-2 (2.7B) Java-
 248 heripi et al. (2023). MSPO utilizes a small, clean meta-dataset ($|D_{meta}| \approx 150$) held out from the
 249 training data for its meta-optimization.

250 **Baselines.** We compare MSPO against a suite of strong and representative baselines: standard
 251 DPO Rafailov et al. (2023), GDPO Furuta et al. (2024) with fixed noisy soft labels, robust loss vari-
 252 ants (cDPO Mitchell (2023) & rDPO Chowdhury et al. (2024)), and a key data-centric competitor,
 253 PerpCorrect-DPO Kong et al. (2024), which uses a static PPLDiff signal for pre-processing.

255 **Evaluation Protocol.** Following standard practice Bai et al. (2022a); Kong et al. (2024), we use
 256 GPT-4 to judge the win rate of trained models against the SFT baseline on a held-out test set. To
 257 ensure statistical robustness, all reported results are the mean and standard deviation over 3 inde-
 258 pendent runs. A detailed description of datasets, noise simulation, model configurations, baseline
 259 implementations, and evaluation protocols is provided in Appendix C.

261 4.2 MAIN RESULTS: ROBUSTNESS TO NOISY PREFERENCES

263 We first evaluate the core hypothesis of our work: that MSPO can achieve superior robustness in the
 264 presence of noisy preference data. We present the win rates of all methods against the SFT baseline
 265 under increasing levels of random label flipping noise. The results for Llama-2-7B and Phi-2 are
 266 summarized in Table 1 and Table 2, respectively.

267 The results across both models and datasets reveal a clear and consistent trend. As expected, the
 268 performance of Vanilla DPO degrades catastrophically as the noise ratio increases. For instance,
 269 on Golden HH with 40% noise, DPO’s win rate on Llama-2-7B plummets to near-random chance
 (53.2%), demonstrating its extreme vulnerability to label noise. While methods incorporating fixed

270 Table 1: Win Rates (%) of Llama-2-7B Against SFT on the Golden HH and OASST1 Test Sets
 271 under Various Levels of Random Label Flipping Noise. Results are reported as mean \pm std over 3
 272 runs. Best results are in **bold**.

273 274 Method	Golden HH					OASST1				
	Clean (0%)	10%	20%	30%	40%	Clean (0%)	10%	20%	30%	40%
Vanilla DPO	97.2 \pm 0.4	92.5 \pm 0.6	82.6 \pm 1.1	68.5 \pm 1.5	53.2 \pm 2.0	97.2 \pm 0.3	96.6 \pm 0.5	92.7 \pm 0.8	90.2 \pm 0.9	86.3 \pm 1.2
GDPO	97.6 \pm 0.3	97.2 \pm 0.4	95.5 \pm 0.5	94.3 \pm 0.6	91.2 \pm 0.9	97.5 \pm 0.2	97.1 \pm 0.3	94.2 \pm 0.6	93.1 \pm 0.7	92.7 \pm 0.8
cDPO	97.4 \pm 0.3	96.0 \pm 0.5	90.9 \pm 0.8	83.2 \pm 1.0	65.6 \pm 1.8	97.7 \pm 0.2	96.2 \pm 0.4	93.6 \pm 0.7	90.6 \pm 0.9	88.0 \pm 1.1
rDPO	97.2 \pm 0.4	96.7 \pm 0.4	95.2 \pm 0.6	93.9 \pm 0.7	90.5 \pm 1.0	97.8 \pm 0.2	95.9 \pm 0.5	93.7 \pm 0.7	92.1 \pm 0.8	90.6 \pm 1.0
PerpCorrect-DPO	97.9 \pm 0.3	97.5 \pm 0.3	96.2 \pm 0.5	95.5 \pm 0.5	94.9 \pm 0.6	98.1 \pm 0.2	96.4 \pm 0.4	94.0 \pm 0.6	94.0 \pm 0.6	93.2 \pm 0.7
MSPO (Ours)	98.4\pm0.2	97.9\pm0.2	96.6\pm0.4	96.3\pm0.4	96.1\pm0.5	98.7\pm0.1	97.4\pm0.3	95.4\pm0.4	94.7\pm0.5	94.4\pm0.5

279
 280 Table 2: Win Rates (%) of Phi-2 (2.7B) Against SFT on the Golden HH and OASST1 Test Sets
 281 under Various Levels of Random Label Flipping Noise. Results are reported as mean \pm std over 3
 282 runs. Best results are in **bold**.

283 284 Method	Golden HH					OASST1				
	Clean (0%)	10%	20%	30%	40%	Clean (0%)	10%	20%	30%	40%
Vanilla DPO	96.5 \pm 0.5	93.2 \pm 0.7	85.6 \pm 1.0	73.1 \pm 1.4	55.0 \pm 1.9	69.1 \pm 1.1	66.9 \pm 1.3	62.6 \pm 1.5	58.4 \pm 1.8	52.4 \pm 2.2
GDPO	97.1 \pm 0.4	97.5 \pm 0.4	96.1 \pm 0.5	94.5 \pm 0.7	85.4 \pm 1.2	68.7 \pm 1.2	67.9 \pm 1.3	63.6 \pm 1.5	59.9 \pm 1.7	53.1 \pm 2.1
cDPO	97.6 \pm 0.3	97.2 \pm 0.4	92.6 \pm 0.8	81.1 \pm 1.2	66.7 \pm 1.8	69.3 \pm 1.1	67.3 \pm 1.3	61.4 \pm 1.6	54.9 \pm 2.0	49.2 \pm 2.5
rDPO	97.0 \pm 0.4	96.5 \pm 0.5	95.7 \pm 0.6	93.3 \pm 0.8	84.6 \pm 1.3	67.2 \pm 1.3	64.0 \pm 1.5	59.5 \pm 1.8	56.5 \pm 1.9	45.2 \pm 2.8
PerpCorrect-DPO	98.2 \pm 0.3	98.2 \pm 0.3	97.1 \pm 0.4	96.7 \pm 0.5	96.4 \pm 0.5	72.6 \pm 0.9	71.3 \pm 1.0	69.0 \pm 1.2	68.3 \pm 1.3	68.5 \pm 1.3
MSPO (Ours)	98.9\pm0.2	98.4\pm0.2	98.0\pm0.3	97.5\pm0.4	97.3\pm0.4	74.8\pm0.8	72.5\pm0.9	71.2\pm1.0	70.6\pm1.1	70.0\pm1.2

290 soft labels (GDPO) or robust loss functions (cDPO, rDPO) offer a degree of protection, their performance still erodes significantly under high noise.

293 The strongest baseline, PerpCorrect-DPO, showcases the power of using PPLDiff for noise correction, maintaining high win rates even at 30-40% noise. This validates the signal’s utility. However, 294 our proposed MSPO consistently and significantly outperforms all baselines across nearly every 295 noise condition. The most striking advantage of MSPO emerges in the high-noise regimes. On 296 Golden HH with 40% noise, MSPO achieves a win rate of 96.1% on Llama-2-7B, a remarkable 297 +42.9% absolute improvement over Vanilla DPO and a solid margin over the strong PerpCorrect- 298 DPO baseline. This demonstrates the core advantage of our dynamic calibration paradigm: MSPO’s 299 ability to learn an adaptive, online correction strategy is substantially more effective than applying a 300 static, heuristic-based correction as a pre-processing step. The performance on the larger and more 301 diverse OASST1 dataset further corroborates these findings, with MSPO maintaining a win rate of 302 94.4% at 40% noise, again leading all other methods.

303 The advantages of MSPO are not limited to a single model architecture. As shown in Table 2, we 304 observe a similar pattern of results with the smaller Phi-2 model. While the absolute win rates on 305 the more challenging OASST1 dataset are lower across all methods for this model, MSPO’s relative 306 advantage remains pronounced. On Golden HH, MSPO again exhibits exceptional resilience, main- 307 taining a 97.3% win rate even at 40% noise, where DPO’s performance has completely collapsed. 308 On OASST1 at 40% noise, MSPO achieves a win rate of 70.0%, significantly higher than the 52.4% 309 of DPO and notably surpassing the 68.5% of PerpCorrect-DPO. This consistent outperformance on 310 a different model architecture further strengthens the evidence for MSPO’s general applicability and 311 robustness as an alignment methodology. Furthermore, direct head-to-head comparisons against the 312 strongest baseline, detailed in Appendix D, confirm that MSPO’s advantage is significant and grows 313 with the noise level.

314 315 4.3 ABLATION STUDIES AND ANALYSIS

316 In this section, we present our most critical ablations. Further studies on the sensitivity to meta- 317 dataset noise and size are deferred to Appendix E. While the main results demonstrate MSPO’s 318 superior performance, this section aims to dissect *why* it is so effective. We conduct targeted abla- 319 tions and analyses to understand the contributions of its key components and to investigate its 320 internal mechanisms.

321 **The Importance of Meta-Learning and Dynamic Signals.** A core question is whether MSPO’s 322 advantage stems from the meta-learning framework, the dynamic PPLDiff signal, or both. To

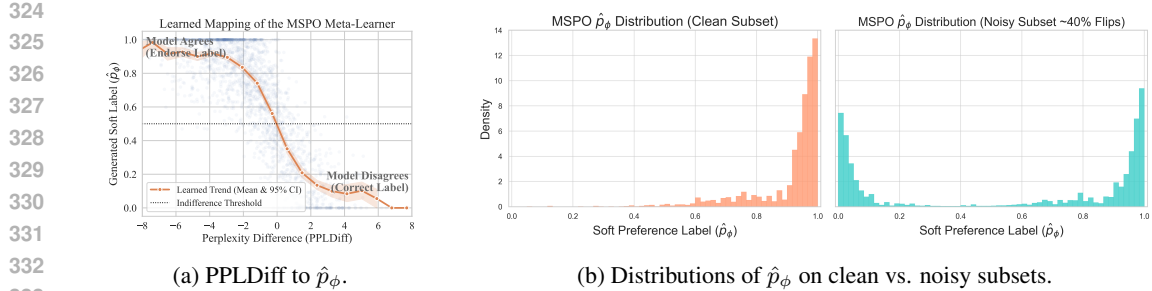


Figure 3: Visual analysis of a trained MSPO meta-learner. (a) It learns a rational, sigmoidal function to map the PPLDiff signal to a soft label. (b) On noisy data, this learned function results in a bimodal distribution of soft labels, effectively separating and correcting a large fraction of mislabeled examples.

disentangle these factors, we conduct a critical ablation study (Table 3) comparing three configurations: (1) PerpCorrect-DPO, which uses a static signal for heuristic-based correction; (2) MSPO-Static, our method using the same static signal, thus isolating the benefit of the learned correction function; and (3) the full MSPO, using a dynamic signal from the evolving model. The results offer a clear two-step insight. First, MSPO-Static outperforms PerpCorrect-DPO, confirming that learning a nuanced mapping is superior to a fixed heuristic. Second, the full MSPO further improves upon MSPO-Static, demonstrating the crucial contribution of the dynamic signal, which allows the correction strategy to adapt as the main model’s own understanding evolves. This synergy of a learned function and a dynamic signal is key to MSPO’s success.

Analysis of the Learned Meta-Learner. To understand *how* MSPO performs noise correction, we visualize the behavior of a trained meta-learner. Figure 3 combines two key analyses. The left panel shows the functional mapping learned by the meta-learner, which translates the PPLDiff signal into a soft label \hat{p}_ϕ . The sensible sigmoidal trend confirms it has learned a rational policy: endorsing model-agreeable preferences ($\text{PPLDiff} \geq 0$), reversing disagreeable ones ($\text{PPLDiff} \leq 0$), and expressing uncertainty when the signal is ambiguous ($\text{PPLDiff} \approx 0$). It learns a *calibrated, continuous function*, not just a simple flip rule.

The right panel of Figure 3 reveals the distributional impact of these learned labels on a noisy dataset (40% flips). On the subset of originally clean pairs, MSPO produces a sharp unimodal distribution near $\hat{p}_\phi = 1.0$. On the subset of pairs with flipped labels, the distribution becomes distinctly bimodal: a large peak near 0.0 reflects successfully identified and corrected labels, while a smaller peak near 1.0 indicates instances where the signal was perhaps ambiguous. This provides compelling visual evidence of MSPO’s core mechanism: it effectively performs a “soft” partitioning of the data, learning to separate trustworthy signals from probable noise at an instance level.

Robustness to More Realistic, Difficulty-Dependent Noise. While random label flipping is a standard benchmark, real-world noise is often not uniformly distributed. Noisy labels may be more prevalent in ‘hard’ or ‘ambiguous’ preference pairs where even human annotators might disagree. To simulate this more realistic scenario, we introduce a difficulty-dependent noise model. We first estimate the difficulty of each preference pair using the absolute log-probability ratio from a powerful, fixed surrogate model. Pairs with low absolute ratios are considered hard, while those with high ratios are easy. We then inject noise asymmetrically: hard pairs

Table 3: Ablation on the signal source and learning mechanism. Win rates (%) are for Llama-2-B on Golden HH (30% noise).

Method Variant	Win Rate (%)
PerpCorrect-DPO (Static)	95.5 ± 0.5
MSPO-Static	95.9 ± 0.4
MSPO (Full, Dynamic)	96.3 ± 0.4

Table 4: Performance under difficulty-dependent noise on Golden HH (Llama-2-7B). MSPO’s advantage widens in this setting.

Method	Win Rate (%)
Vanilla DPO	61.3 ± 1.8
cDPO	75.8 ± 1.2
PerpCorrect-DPO	93.1 ± 0.7
MSPO (Ours)	95.2 ± 0.5

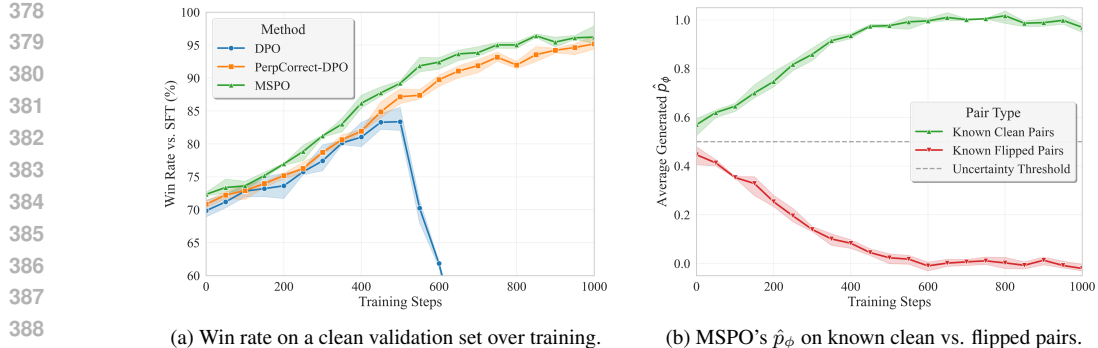


Figure 4: Training dynamics on Golden HH with 30% noise. (a) MSPO demonstrates a more stable and effective learning trajectory compared to baselines. (b) The MSPO meta-learner rapidly learns to differentiate between clean and flipped labels, assigning corrective soft labels early in training, thus avoiding self-reinforcing errors and enabling a positive feedback loop.

are flipped with a high probability (e.g., 40%), while easy pairs are flipped with a low probability (e.g., 10%), creating a challenging testbed where the most ambiguous signals are the most likely to be corrupted.

The results in Table 4 are illuminating. The performance gap between MSPO and the strong PerpCorrect-DPO baseline *widens* in this setting compared to the uniform random noise experiments. PerpCorrect-DPO, relying on a fixed heuristic, struggles more when the PPLDiff signal is inherently ambiguous for the hard (and most frequently flipped) pairs. In contrast, MSPO’s meta-learner, having been trained to interpret the entire spectrum of PPLDiff values, can learn a more sophisticated policy. It can learn to be more conservative and assign soft labels closer to 0.5 for these ambiguous cases, or leverage subtle patterns in the signal that a fixed threshold would miss. This result strongly suggests that MSPO’s adaptive, learned approach is not just a marginal improvement, but a fundamentally more robust paradigm for handling the complex, non-uniform noise often encountered in real-world preference data.

4.4 ANALYSIS OF TRAINING DYNAMICS

A potential concern for any method that relies on a signal from an evolving model is the risk of self-reinforcing errors, where an initially biased model provides poor signals, leading to further degradation. To investigate whether MSPO suffers from this issue and to better understand its learning process, we analyze its training dynamics on Golden HH with 30% noise, comparing it against key baselines.

Figure 4 presents two key views into the training process. The left panel plots the win rate on a clean, held-out validation set as a function of training steps. While all methods start from the same SFT model, their learning trajectories diverge significantly. DPO’s performance initially rises but then quickly collapses as it overfits to the noisy labels. PerpCorrect-DPO shows a much more stable trajectory, demonstrating the benefit of noise correction. However, MSPO not only reaches a higher final win rate but also exhibits a stable and monotonically improving performance curve, suggesting a more robust and efficient learning process.

The right panel of Figure 4 provides a direct window into the meta-learner’s behavior and offers a compelling explanation for this stability. It tracks the average soft label \hat{p}_ϕ that MSPO assigns to two subsets of the training data: the known clean pairs and the known flipped pairs. The result is striking: remarkably early in the training process, the meta-learner learns to distinguish between these two groups. The average \hat{p}_ϕ for clean pairs rapidly climbs towards 1.0, while the average for flipped pairs quickly drops towards 0.0. This demonstrates that the dynamic PPLDiff signal, even from a partially trained model, is sufficiently informative for the meta-learner to establish a correct corrective policy. Rather than a vicious cycle of self-reinforcing errors, MSPO creates a virtuous cycle: the main model provides a useful signal, the meta-learner uses it to clean the training objective, which in turn helps the main model improve more effectively, leading to even better signals. This positive feedback loop is the core reason for MSPO’s robust and stable learning dynamics.

432 **5 RELATED WORK**

434 **LLM Alignment with Human Preferences.** Aligning Large Language Models (LLMs) with hu-
 435 man values is a central challenge for their responsible deployment Ouyang et al. (2022); Stiennon
 436 et al. (2020). Early paradigms often involved a two-stage process: first training an explicit reward
 437 model on human preferences, then fine-tuning the LLM using reinforcement learning (RL) to max-
 438 imize this reward Christiano et al. (2017); Ziegler et al. (2019). More recently, Direct Preference
 439 Optimization (DPO) Rafailov et al. (2023) and its variants have gained prominence by directly opti-
 440 mizing a policy against preference data, bypassing the need for an intermediate reward model. While
 441 effective, these methods typically treat preferences as binary signals, failing to capture the nuanced
 442 strength or certainty of human judgments. To address this, works like Geometric-Averaged DPO
 443 (GDPO) have been proposed to incorporate soft preference labels Furuta et al. (2024). However, the
 444 effectiveness of such approaches is fundamentally limited by the quality of these labels, a challenge
 445 our work directly confronts by learning to generate them adaptively from noisy data.

446 **Addressing Noisy Preferences in LLM Alignment.** The presence of noise in preference datasets
 447 is a well-recognized obstacle to robust alignment Gao et al. (2024); Casper et al. (2023). Existing
 448 mitigation strategies can be broadly categorized. One line of work focuses on robust loss functions,
 449 such as Conservative DPO (cDPO) Mitchell (2023) and Robust DPO (rDPO) Chowdhury et al.
 450 (2024), which adjust the DPO objective based on an estimated global noise ratio. While beneficial,
 451 these methods lack instance-level adaptability. A second, data-centric line of work aims to correct
 452 noisy labels as a pre-processing step. A notable example is Perplexity-aware Correction (PerpCor-
 453 rect) Kong et al. (2024), which leverages perplexity differences (PPLDiff) from a *fixed surrogate*
 454 *model* to identify and flip potentially mislabeled pairs based on heuristic rules. MSPO shares the
 455 insight of using PPLDiff as a noise indicator but fundamentally differs in its approach: instead of
 456 applying a static, one-time correction, MSPO learns a *dynamic, adaptive function* that continuously
 457 refines soft preference labels throughout the training process, using signals from the evolving main
 458 model itself.

459 **Meta-learning for Robust Label Correction.** Our work is also inspired by a rich body of liter-
 460 ature on meta-learning for robust training in the presence of noisy labels, predominantly in clas-
 461 sification tasks Ren et al. (2018); Shu et al. (2019); Wu et al. (2021); Wang et al. (2020). These
 462 methods typically train a meta-learner on a small, clean dataset to learn a strategy—such as a sam-
 463 ple re-weighting function or a label correction model—that improves the main task’s performance
 464 on the noisy training set. For instance, Meta-Weight-Net Shu et al. (2019) learns a function to as-
 465 sign weights to training samples based on their loss values. While these works demonstrate the
 466 power of meta-learning for handling label noise, its application to the unique challenges of LLM
 467 preference alignment has been largely unexplored. MSPO bridges this gap by pioneering the use of
 468 meta-learning to optimize *soft preference labels* (rather than simple classification labels or sample
 469 weights) and by leveraging a *dynamic, model-intrinsic signal* (PPLDiff from the evolving policy) as
 470 the core input to the meta-learner, a concept not present in prior meta-learning literature for label
 471 correction.

472 **6 CONCLUSION**

473 In this work, we addressed the critical challenge of noisy preferences by introducing Dynamic Pref-
 474 erence Calibration, a new paradigm for robust Large Language Model alignment. We argued that
 475 existing methods based on static corrections are insufficient and introduced Meta Soft Preference
 476 Optimization (MSPO), a framework that operationalizes our paradigm by meta-learning to derive
 477 adaptive soft labels from dynamic, model-intrinsic signals. By learning to translate perplexity dif-
 478 ferences into calibrated preference strengths, MSPO creates a virtuous cycle that allows the noise
 479 correction strategy to co-evolve with the model’s own improving understanding. Our extensive
 480 experiments and in-depth analyses demonstrate that MSPO establishes a new state-of-the-art in robust
 481 LLM alignment, consistently and significantly outperforming strong baselines, particularly in high-
 482 noise and more realistic, difficulty-dependent noise scenarios. This work highlights the promise of
 483 meta-learning as a powerful paradigm for learning to calibrate preferences, paving the way for more
 484 reliable and robust alignment techniques.

486 ETHICS STATEMENT
487488 In accordance with ICLR policy, we disclose that large language models (LLMs) were employed
489 as writing assistants during the preparation of this paper. Their primary function was to support
490 grammar correction and language refinement, with the goal of improving the overall readability of
491 the manuscript. All core ideas and analyses were conceived and developed solely by the human
492 authors, who assume full responsibility for the final content of the paper.493
494 REFERENCES
495496 Dario Amodei, Chris Olah, Jacob Steinhardt, Paul Christiano, John Schulman, and Dan Mané. Con-
497 crete problems in ai safety. *arXiv preprint arXiv:1606.06565*, 2016.498 Rohan Anil, Andrew M. Dai, Orhan Firat, Melvin Johnson, Dmitry Lepikhin, Alexandre Passos,
499 Siamak Shakeri, Emanuel Taropa, Paige Bailey, Zhifeng Chen, Eric Chu, Jonathan H. Clark,
500 Laurent El Shafey, Yanping Huang, Kathy Meier-Hellstern, Gaurav Mishra, Erica Moreira, Mark
501 Omernick, Kevin Robinson, Sebastian Ruder, Yi Tay, Kefan Xiao, Yapei Xu, Yujing Zhang, Gus-
502 tavo H. Abrego, Junwhan Ahn, Jacob Austin, Paul Barham, Jan Botha, James Bradbury, Srivatsan
503 Brahma, Kevin Brooks, Michele Catasta, Yong Cheng, Colin Cherry, Christopher A. Choquette-
504 Choo, Aakanksha Chowdhery, Clement Crepy, Shachi Dave, Mostafa Dehghani, Sunayana Dev,
505 Jacob Devlin, Mark Diaz, Nan Du, Vyrill Feinberg, Fangxia Feng, Vlad Fienber, Markus Fre-
506 itag, Xavier Garcia, Sebastian Gehrmann, Lucas Gonzalez, Guy Gur-Ari, Steven Hand, Hossein
507 Hashemi, Le Hou, Jacob Howland, Andrea Hu, Joanna Huitou, Michael Isard, Abe Ittycheriah,
508 Matthew Jagielski, Wenhao Jia, Kathleen Kenealy, Maxim Krikun, Shridhar Kudugunta, Chang
509 Lan, Katherine Lee, Benjamin Lee, Eric Li, Music Li, Wei Li, Ya Li, Jian Li, Hye-Won Lim,
510 Hanzhi Lin, Zhongguo Liu, Frederick Liu, Machel Maggioni, Ankur Mahendru, Julian Maynez,
511 Vedant Misra, Maysam Moussallem, Zachary Nado, John Nham, Eric Ni, Andrew Nystrom, Ali-
512 cia Parrish, Marie Pellar, Martin Polacek, Alex Polozov, Rebeca Pope, Siyuan Qiao, Emily Reif,
513 Bryan Richter, Parker Riley, A. C. Ros, Aurko Roy, Benjamin Saeta, Rajkumar Samuel, Renee
514 Shelby, Ambrose Slone, Daniel Smilkov, David R. So, Daniel Sohn, Simon Tokumine, Dasha
515 Valter, Vinay Vasudevan, Kiran Vodrahalli, Xuezhi Wang, Pidong Wang, Zirui Wang, John Wiet-
516 ing, Yuhuai Wu, Kelvin Xu, Keli Xu, Lier Xue, Pan Yin, Jiahui Yu, Qiao Zhang, Steven Zheng,
517 Ce Zheng, Wensheng Zhou, Slav Petrov, and Yonghui Wu. Palm 2 technical report. Technical
518 report, arXiv preprint, 2023.519 Amanda Askell, Yuntao Bai, Anna Chen, Dawn Drain, Deep Ganguli, Tom Henighan, Andy Jones,
520 Nicholas Joseph, Ben Mann, Nova DasSarma, et al. A general language assistant as a laboratory
521 for alignment. *arXiv preprint arXiv:2112.00861*, 2021.522 Yuntao Bai, Andy Jones, Kamal Ndousse, Amanda Askell, Anna Chen, Nova DasSarma, Dawn
523 Drain, Stanislav Fort, Deep Ganguli, Tom Henighan, Nicholas Joseph, Saurav Kadavath, Jackson
524 Kernion, Tom Conerly, Sheer El-Showk, Nelson Elhage, Zac Hatfield-Dodds, Danny Hernan-
525 dez, Tristan Hume, Scott Johnston, Shauna Kravec, Liane Lovitt, Neel Nanda, Catherine Olsson,
526 Dario Amodei, Tom Brown, Jack Clark, Sam McCandlish, Chris Olah, Ben Mann, and Jared Ka-
527 plan. Training a helpful and harmless assistant with reinforcement learning from human feedback.
528 *arXiv preprint arXiv:2204.05862*, 2022a.529 Yuntao Bai, Saurav Kadavath, Sandipan Kundu, Amanda Askell, Jackson Kernion, Andy Jones,
530 Anna Chen, Anna Goldie, Azalia Mirhoseini, Cameron McKinnon, Carol Chen, Catherine Ols-
531 son, Christopher Olah, Danny Hernandez, Dawn Drain, Deep Ganguli, Dustin Li, Eli Tran-
532 Johnson, Ethan Perez, Jamie Kerr, Jared Mueller, Jeffrey Ladish, Joshua Landau, Kamal Ndousse,
533 Kamile Lukosuite, Liane Lovitt, Michael Sellitto, Nelson Elhage, Nicholas Schiefer, Noemi Mer-
534 cado, Nova DasSarma, Robert Lasenby, Robin Larson, Sam Ringer, Scott Johnston, Shauna
535 Kravec, Sheer El Showk, Stanislav Fort, Tamera Lanham, Timothy Telleen-Lawton, Tom Con-
536 erly, Tom Henighan, Tristan Hume, Samuel R. Bowman, Zac Hatfield-Dodds, Ben Mann, Dario
537 Amodei, Nicholas Joseph, Sam McCandlish, Tom Brown, and Jared Kaplan. Constitutional ai:
538 Harmlessness from ai feedback. *arXiv preprint arXiv:2212.08073*, 2022b.539 Tom B. Brown, Benjamin Mann, Nick Ryder, Melanie Subbiah, Jared Kaplan, Prafulla Dhari-
540 wal, Arvind Neelakantan, Pranav Shyam, Girish Sastry, Amanda Askell, Sandhini Agarwal,

540 Ariel Herbert-Voss, Gretchen Krueger, Tom Henighan, Rewon Child, Aditya Ramesh, Daniel M.
 541 Ziegler, Jeffrey Wu, Clemens Winter, Christopher Hesse, Mark Chen, Eric Sigler, Mateusz Litwin,
 542 Scott Gray, Benjamin Chess, Jack Clark, Christopher Berner, Sam McCandlish, Alec Radford,
 543 Ilya Sutskever, and Dario Amodei. Language models are few-shot learners. *arXiv preprint*
 544 *arXiv:2005.14165*, 2020.

545 Stephen Casper, Xander Davies, Claudia Shi, Thomas Krendl Gilbert, Jérémie Scheurer, Javier
 546 Rando, Rachel Freedman, Tomasz Korbak, David Lindner, Pedro Freire, et al. Open problems
 547 and fundamental limitations of reinforcement learning from human feedback. *arXiv preprint*
 548 *arXiv:2307.15217*, 2023.

550 Sayak Ray Chowdhury, Anush Kini, and Nagarajan Natarajan. Provably robust dpo: Aligning
 551 language models with noisy feedback. *arXiv preprint arxiv:2403.00409*, 2024.

552 Paul Christiano, Jan Leike, Tom B. Brown, Miljan Martic, Shane Legg, and Dario Amodei. Deep
 553 reinforcement learning from human preferences. *arXiv preprint arXiv:1706.03741*, 2017.

555 Hiroki Furuta, Kuang-Huei Lee, Shixiang Shane Gu, Yutaka Matsuo, Aleksandra Faust, Heiga Zen,
 556 and Izzeddin Gur. Geometric-averaged preference optimization for soft preference labels. In
 557 *NeurIPS*, volume 37, pp. 57076–57114, 2024.

559 Yang Gao, Dana Alon, and Donald Metzler. Impact of preference noise on the alignment perfor-
 560 mance of generative language models. *arXiv preprint arXiv:2404.09824*, 2024.

561 Mojan Javaheripi, Sébastien Bubeck, Marah Abdin, Jyoti Aneja, Sébastien Bubeck, Caio
 562 César Teodoro Mendes, Weizhu Chen, Allie Del Giorno, Ronen Eldan, Sivakanth Gopi, et al.
 563 Phi-2: The surprising power of small language models. *Microsoft Research Blog*, 1(3):3, 2023.

565 Keyi Kong, Xilie Xu, Di Wang, Jingfeng Zhang, and Mohan S Kankanhalli. Perplexity-aware
 566 correction for robust alignment with noisy preferences. In *NeurIPS*, volume 37, pp. 28296–28321,
 567 2024.

568 Andreas Köpf, Yannic Kilcher, Dimitri Von Rütte, Sotiris Anagnostidis, Zhi Rui Tam, Keith
 569 Stevens, Abdullah Barhoum, Duc Nguyen, Oliver Stanley, Richárd Nagyfi, et al. Openassis-
 570 tant conversations-democratizing large language model alignment. In *NeurIPS*, volume 36, pp.
 571 47669–47681, 2023.

573 Harrison Lee, Samrat Phatale, Hassan Mansoor, Thomas Mesnard, Johan Ferret, Kellie Lu, Colton
 574 Bishop, Ethan Hall, Victor Carbune, Abhinav Rastogi, and Sushant Prakash. Rlaif: Scaling re-
 575 enforcement learning from human feedback with ai feedback. *arXiv preprint arXiv:2309.00267*,
 576 2023.

577 Xize Liang, Chao Chen, Jie Wang, Yue Wu, Zhihang Fu, Zhihao Shi, Feng Wu, and Jieping
 578 Ye. Robust preference optimization with provable noise tolerance for llms. *arXiv preprint*
 579 *arxiv:2404.04102*, 2024.

581 Ilya Loshchilov and Frank Hutter. Decoupled weight decay regularization. *arXiv preprint*
 582 *arXiv:1711.05101*, 2017.

584 Eric Mitchell. A note on dpo with noisy preferences & relationship to ipo, 2023. URL <https://ericmitchell.ai/cdpo.pdf>.

586 Long Ouyang, Jeff Wu, Xu Jiang, Diogo Almeida, Carroll L. Wainwright, Pamela Mishkin, Chong
 587 Zhang, Sandhini Agarwal, Katarina Slama, Alex Ray, John Schulman, Jacob Hilton, Fraser Kel-
 588 ton, Luke Miller, Maddie Simens, Amanda Askell, Peter Welinder, Paul Christiano, Jan Leike,
 589 and Ryan Lowe. Training language models to follow instructions with human feedback. *arXiv*
 590 *preprint arXiv:2203.02155*, 2022.

592 Rafael Rafailev, Archit Sharma, Eric Mitchell, Christopher D Manning, Stefano Ermon, and Chelsea
 593 Finn. Direct preference optimization: Your language model is secretly a reward model. In
 594 *NeurIPS*, 2023.

594 Mengye Ren, Wenyuan Zeng, Bin Yang, and Raquel Urtasun. Learning to reweight examples for
 595 robust deep learning. In *International conference on machine learning*, pp. 4334–4343. PMLR,
 596 2018.

597

598 Jun Shu, Qi Xie, Lixuan Yi, Qian Zhao, Sanping Zhou, Zongben Xu, and Deyu Meng. Meta-weight-
 599 net: Learning an explicit mapping for sample weighting. In *NeurIPS*, volume 32, 2019.

600 Nisan Stiennon, Long Ouyang, Jeff Wu, Daniel M. Ziegler, Ryan Lowe, Chelsea Voss, Alec Radford,
 601 Dario Amodei, and Paul Christiano. Learning to summarize from human feedback. *arXiv preprint*
 602 *arXiv:2009.01325*, 2020.

603

604 Hugo Touvron, Louis Martin, Kevin Stone, Peter Albert, Amjad Almahairi, Yasmine Babaei, Niko-
 605 lay Bashlykov, Soumya Batra, Prajjwal Bhargava, Shruti Bhosale, Dan Bikel, Lukas Blecher,
 606 Cristian Canton Ferrer, Moya Chen, Guillem Cucurull, David Esiobu, Jude Fernandes, Jeremy
 607 Fu, Wenyin Fu, Brian Fuller, Cynthia Gao, Vedanuj Goswami, Namana Goyal, Anthony Hartshorn,
 608 Saghar Hosseini, Rui Hou, Hakan Inan, Marcin Kardas, Viktor Kerkez, Madian Khabsa, Isabel
 609 Kloumann, Artem Korenev, Punit Singh Koura, Marie-Anne Lachaux, Thibaut Lavril, Jenya Lee,
 610 Diana Liskovich, Yinghai Lu, Yuning Mao, Xavier Martinet, Todor Mihaylov, Pushkar Mishra,
 611 Igor Molybog, Yixin Nie, Andrew Poulton, Jeremy Reizenstein, Rashi Rungta, Kalyan Saladi,
 612 Alan Schelten, Ruan Silva, Eric Michael Smith, Ranjan Subramanian, Xiaoqing Ellen Tan, Binh
 613 Tang, Ross Taylor, Adina Williams, Jian Xiang Kuan, Puxin Xu, Zheng Yan, Iliyan Zarov, Yuchen
 614 Zhang, Angela Fan, Melanie Kambadur, Sharan Narang, Aurelien Rodriguez, Robert Stojnic,
 615 Sergey Edunov, and Thomas Scialom. Llama 2: Open foundation and fine-tuned chat models,
 616 2023.

617

618 Zhen Wang, Guosheng Hu, and Qinghua Hu. Training noise-robust deep neural networks via meta-
 619 learning. In *CVPR*, pp. 4524–4533, 2020.

620

621 Yichen Wu, Jun Shu, Qi Xie, Qian Zhao, and Deyu Meng. Learning to purify noisy labels via meta-
 622 soft label corrector. In *AAAI*, volume 35, pp. 10388–10396, 2021.

623

624 Sen Zhao, Mahdi Milani Fard, Harikrishna Narasimhan, and Maya Gupta. Metric-optimized exam-
 625 ple weights. In *ICML*, pp. 7533–7542, 2019.

626

627

628 **A ALGORITHM FOR MSPO TRAINING**

629

630 The complete training procedure for MSPO is detailed in Algorithm 1. The algorithm outlines the
 631 iterative, three-step bilevel optimization process for updating the main LLM parameters θ and the
 632 meta-learner parameters ϕ .

633

634

635 **B THEORETICAL ANALYSIS OF MSPO**

636

637 This section provides a theoretical lens through which to understand MSPO’s mechanism. We first
 638 interpret the bilevel optimization as learning an implicit weighting scheme and then present a high-
 639 level generalization bound for the learned meta-policy.

640

641 **B.1 IMPLICIT WEIGHTING SCHEME IN MSPO**

642

643 The meta-learning process in MSPO can be viewed as learning an implicit, adaptive scheme for re-
 644 interpreting or re-weighting noisy training preferences. The update to the meta-learner’s parameters,
 645 ϕ , is driven by its ability to produce soft labels that guide the main LLM towards better performance
 on a clean meta-dataset.

646

647 The update rule for ϕ at step t is given by gradient descent on the meta-loss:

$$\phi^{(t+1)} = \phi^{(t)} - \eta_{\text{meta}} \nabla_{\phi} \mathcal{L}_{\text{meta}}(\phi^{(t)}). \quad (13)$$

Using the chain rule, the meta-gradient $\nabla_{\phi}\mathcal{L}_{\text{meta}}(\phi^{(t)})$ can be expanded as:

$$\nabla_{\phi} \mathcal{L}_{\text{meta}} = \mathbb{E}_{\mathcal{B}_{\text{meta}}} \left[\nabla_{\theta_{\text{virtual}}} \mathcal{L}_{\text{DPO}}(\pi_{\theta_{\text{virtual}}(\phi^{(t)})}) \cdot \frac{d\theta_{\text{virtual}}(\phi^{(t)})}{d\phi^{(t)}} \right]. \quad (14)$$

The term $\frac{d\theta_{\text{virtual}}(\phi^{(t)})}{d\phi^{(t)}}$ represents how the virtual parameters change with respect to the meta-parameters. Substituting the definition of θ_{virtual} from Eq. 8, we get:

$$\frac{d\theta_{\text{virtual}}(\phi^{(t)})}{d\phi^{(t)}} = -\alpha \nabla_\phi \nabla_\theta \mathcal{L}_{\text{main}}^{\text{virtual}}(\theta; \phi^{(t)})|_{\theta=\theta^{(t)}}. \quad (15)$$

The Hessian-vector product in this term connects the meta-learner's parameters ϕ to the main model's update. Specifically, the gradient ∇_ϕ operates on $\mathcal{L}_{\text{main}}^{\text{virtual}}$ through the generated soft labels $\hat{p}_{\phi^{(t)}} = V(\text{PPLDiff}^{(t)}; \phi^{(t)})$.

This structure implies that the meta-learner parameters ϕ are updated in a direction that rewards the generation of soft labels \hat{p}_ϕ which, when used to train the virtual LLM on the noisy batch $\mathcal{B}_{\text{train}}$, lead to improved performance (lower \mathcal{L}_{DPO}) on the clean meta-batch $\mathcal{B}_{\text{meta}}$. In essence, training instances (via their PPLDiff signals) that are transformed by $V(\cdot; \phi)$ into “beneficial” soft labels—as judged by their downstream utility for clean alignment—will exert a stronger and more favorable influence on the meta-learner’s update. This can be seen as an implicit, adaptive re-weighting of the training preferences based on their alignment utility.

702 B.2 GENERALIZATION BOUND FOR MSPO
703

704 We provide a high-level generalization bound for MSPO, drawing inspiration from standard analyses
705 in meta-learning and learning with noisy labels Zhao et al. (2019). Let $R_{\text{clean}}(\phi)$ be the true expected
706 risk (e.g., expected \mathcal{L}_{DPO} on the true clean preference distribution P_{clean}) of the main LLM policy
707 that is trained using the soft labels generated by the meta-learner $V(\cdot; \phi)$. Let $\hat{R}_{\text{meta}}(\phi) = \mathcal{L}_{\text{meta}}(\phi)$
708 be the empirical risk on the clean meta-dataset $\mathcal{D}_{\text{meta}}$ of size M . We aim to bound the generalization
709 gap $|R_{\text{clean}}(\phi^*) - \hat{R}_{\text{meta}}(\phi^*)|$, where ϕ^* is the set of parameters learned by MSPO.
710

711 **Assumptions.** We make the following standard assumptions: 1) The meta-learner’s parameter
712 space Φ is bounded. 2) The DPO loss is bounded, $\mathcal{L}_{\text{DPO}} \in [0, B_{\text{loss}}]$. 3) The meta-dataset $\mathcal{D}_{\text{meta}}$
713 consists of M i.i.d. samples from P_{clean} .
714

715 **Theorem (MSPO Generalization Bound - Informal).** Let $\phi^* = \arg \min_{\phi \in \Phi} \hat{R}_{\text{meta}}(\phi)$ be the
716 parameters learned by minimizing the meta-loss. Then, for any $\delta > 0$, with probability at least $1 - \delta$
717 over the random draw of $\mathcal{D}_{\text{meta}}$:

$$718 R_{\text{clean}}(\phi^*) \leq \hat{R}_{\text{meta}}(\phi^*) + \mathcal{O} \left(\sqrt{\frac{\text{Comp}(\mathcal{F}_{\Phi}) + \log(1/\delta)}{M}} \right), \quad (16)$$

721 where $\text{Comp}(\mathcal{F}_{\Phi})$ is a measure of the complexity of the function class induced by the meta-learner,
722 for instance, its Rademacher complexity. For a parametric model like a neural network for $V(\cdot; \phi)$,
723 this complexity term is related to its size and depth.
724

725 **Implication.** This bound indicates that the performance of the MSPO-trained meta-learner on
726 unseen clean data is controlled by its empirical performance on the meta-dataset and the complexity
727 of the meta-learner itself. As the size of the clean meta-dataset M increases, the generalization gap
728 shrinks, ensuring that minimizing the meta-loss on $\mathcal{D}_{\text{meta}}$ leads to a meta-learner that is effective
729 on the true clean data distribution. This provides theoretical justification for MSPO’s data-driven
730 approach to learning a robust label correction policy.
731

732 C IMPLEMENTATION DETAILS
733

734 This section provides comprehensive details of our experimental setup to ensure full reproducibility.
735

736 **Model Configurations.** Our experiments are based on two publicly available pretrained language
737 models: **Llama-2-7B-Chat-HF** Touvron et al. (2023) and **Phi-2** Javaheripi et al. (2023). For each
738 base model, we first perform supervised fine-tuning (SFT) on the clean ‘chosen’ responses from the
739 training split of the respective dataset (Golden HH or OASST1) for one epoch. This SFT model
740 serves as the starting point ($\pi_{\theta(0)}$) for all subsequent alignment methods and also as the fixed refer-
741 ence policy (π_{ref}) in all DPO-style loss calculations.
742

743 **Meta-Learner Architecture ($V(\cdot; \phi)$).** The meta-learner in MSPO is a simple yet effective Multi-
744 Layer Perceptron (MLP). It consists of an input layer taking a single scalar (the PPLDiff value), two
745 hidden layers with 128 units each and ReLU activation functions, and a final output layer with a
746 single neuron and a Sigmoid activation. The sigmoid function ensures the output \hat{p}_{ϕ} is constrained to
747 the range $[0, 1]$. We found this simple architecture to be robust and effective across all experiments.
748 Before being fed to the MLP, the PPLDiff values are z-score normalized based on statistics computed
749 from the first 1000 training samples.
750

751 **PPLDiff Computation.** As defined in Eq. 4, the Perplexity Difference is calculated based on
752 the log-perplexity of the concatenated prompt and response sequences. We use the model’s standard
753 causal language modeling loss (cross-entropy) to compute the log-perplexity. To account for variable
754 response lengths, the loss for each sequence is normalized by the number of tokens in the response
755 part (y_w or y_l). For MSPO, the PPLDiff is computed dynamically at each step using the current
main LLM $\pi_{\theta(t)}$. For the PerpCorrect-DPO baseline, it is pre-computed once using the fixed SFT
model as the surrogate.
756

756 **Baseline Configurations.** We provide specifics for our baseline implementations to ensure clarity
 757 and fairness:

759 • **GDPO:** We use an initial soft label of $\hat{p}_0 = 0.9$ for clean preferences. When a label is
 760 flipped for noise simulation, this soft label is correspondingly flipped to $1 - \hat{p}_0 = 0.1$.

761 • **cDPO & rDPO:** These methods require an estimate of the noise ratio ϵ . To ensure a fair
 762 comparison, this ratio is estimated using the same clean meta-dataset D_{meta} that MSPO
 763 uses. For example, for a 30% noisy dataset, we would inform the algorithm that the true
 764 noise ratio is 0.3, simulating a scenario where a small clean set is available for such esti-
 765 mations. We use the official implementations provided by the original authors.

766 • **PerpCorrect-DPO:** We use the implementation from the original paper. The correction is
 767 performed as a pre-processing step. A preference label is flipped if the PPLDiff computed
 768 by the fixed SFT model is greater than a threshold τ . This threshold is tuned on the clean
 769 D_{meta} to maximize accuracy.

770 **Training Hyperparameters.** Key hyperparameters for both the main LLM alignment and the
 771 MSPO meta-learner are summarized in Table 5. We used the AdamW optimizer Loshchilov &
 772 Hutter (2017) for all models. The learning rate for the main LLM was carefully tuned for each
 773 model, while the meta-learner used a consistent, higher learning rate. All alignment methods were
 774 trained for 1 epoch over their respective training datasets.

776 Table 5: Key Hyperparameters for LLM Alignment and MSPO Meta-learner.

778 Hyperparameter	779 LLM Alignment (π_θ)	779 MSPO Meta-learner ($V(\cdot; \phi)$)
779 Optimizer	AdamW	AdamW
780 Learning Rate (α, η_{meta})	5e-7 (Llama-2) / 1e-6 (Phi-2)	1e-4
781 Effective Batch Size	64 pairs	64 pairs (meta-update)
782 β in DPO loss	0.1	N/A
783 Warm-up Steps	100	N/A
784 Weight Decay	0.01	0.0
785 Gradient Clipping Norm	1.0	Not applied

787 **Evaluation Details.** Evaluation is performed on a held-out test set of 1,000 prompts randomly
 788 sampled from the official test splits of each dataset. For automated evaluation, we used the OpenAI
 789 API with the ‘gpt-4-0613’ model. We employed a standard pairwise comparison prompt asking
 790 the judge to rate which response was better, with ties excluded from the win rate calculation. The
 791 positions of the two responses (A or B) were randomized to mitigate positional bias.

792 **Computational Resources.** All experiments were conducted on a cluster of NVIDIA A40 (48GB)
 793 GPUs. Training Llama-2-7B with MSPO for one epoch on the Golden HH dataset (approx. 80k
 794 pairs) takes approximately 10-12 hours on 4 A100 GPUs. The bilevel optimization introduces an
 795 approximate 25-30% computational overhead compared to a standard DPO training run due to the
 796 virtual gradient computation and the meta-learner updates.

798 D EXTENDED EVALUATION DETAILS

801 This section provides further details on our evaluation to enhance transparency and offer additional
 802 perspectives on model performance.

803 **Head-to-Head Win Rates.** While win rates against a fixed SFT baseline (as reported in the main
 804 paper) are useful for measuring overall improvement, direct head-to-head comparisons between the
 805 top-performing methods can offer a clearer picture of their relative strengths. We conducted a head-
 806 to-head evaluation between our full MSPO model and the strongest baseline, PerpCorrect-DPO,
 807 using GPT-4 as the judge. The models were trained on Golden HH with varying levels of noise.

809 Table 6 shows the results. The win rate is calculated from MSPO’s perspective as ‘(MSPO Wins)
 / (MSPO Wins + PerpCorrect-DPO Wins)’, excluding ties. The results confirm the findings from

810 the main paper: in the clean setting, the two methods perform comparably, with a win rate close to
 811 50%. However, as the noise level increases, MSPO’s advantage becomes increasingly pronounced.
 812 At 40% noise, MSPO wins against PerpCorrect-DPO nearly two-thirds of the time. This direct
 813 comparison provides strong evidence that MSPO’s adaptive, online correction mechanism confers a
 814 tangible and significant advantage over static pre-processing methods in noisy environments.
 815

816 Table 6: Head-to-head win rates (%) of MSPO against PerpCorrect-DPO on Golden HH (Llama-2-
 817 7B). A rate $\geq 50\%$ indicates MSPO is preferred.

818 Training Noise Ratio	819 MSPO Win Rate vs. PerpCorrect-DPO (%)
820 0% (Clean)	821 51.2 ± 1.5
822 20%	58.6 ± 2.1
40%	64.3 ± 2.5

823
 824 **LLM Judge Protocol and Bias Mitigation.** Our use of GPT-4 as an automated evaluator follows
 825 established community norms. To ensure fairness and minimize potential biases, we implemented
 826 several best practices:
 827

- 828 • **Anonymization:** The judge was never aware of which model produced which response.
 829 The models were simply labeled “Response A” and “Response B”.
- 830 • **Positional Randomization:** The order of the responses (i.e., whether a model’s output
 831 appeared as A or B) was randomized for each evaluation query to mitigate positional bias,
 832 where judges may have an inherent preference for the first or second response.
- 833 • **Forced Choice with Tie Option:** We used a prompt that asked for a comparative judgment
 834 (A is better, B is better) but also included an option for ties (“Both are of similar quality”).
 835 This is crucial for obtaining a clean win/loss signal. All ties were excluded from the win
 836 rate calculations.
- 837 • **Prompting for Justification:** The judge was required to provide a brief justification for
 838 its choice. While not systematically analyzed, a manual review of these justifications con-
 839 firmed that the model was generally applying reasonable criteria related to helpfulness,
 840 clarity, and detail.

841 While no automated evaluator is perfect, these steps were taken to ensure our evaluation was as
 842 robust and unbiased as possible. The full prompt template used for evaluation is provided in a
 843 subsequent section.

844 E ADDITIONAL ABLATION STUDIES

845 To further characterize the behavior and robustness of MSPO, we conducted several additional ab-
 846 lation studies.

847 **Sensitivity to Noise in the Meta-Dataset.** A core assumption of our framework is the availability
 848 of a small, *clean* meta-dataset D_{meta} . To test how robust MSPO is to violations of this assumption,
 849 we conducted an experiment where we intentionally injected random label flipping noise into D_{meta}
 850 itself. We then re-ran our main experiment on Golden HH with 30% noise in the primary training
 851 set and observed the impact on MSPO’s final performance.

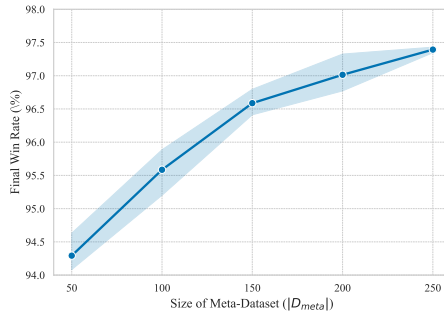
852 The results, shown in Table 7, indicate that MSPO’s performance degrades gracefully as the quality
 853 of the meta-dataset decreases. Even with 10% noise in the meta-dataset—a challenging scenario
 854 where the meta-learner receives conflicting supervisory signals—MSPO still achieves a win rate of
 855 95.1%. This is significantly higher than Vanilla DPO (68.5%) and remains competitive with the
 856 strongest baseline, PerpCorrect-DPO (95.5%), which benefits from a perfectly clean set for tuning
 857 its threshold. This suggests that the meta-learning process is inherently robust; as long as the signal
 858 from the meta-dataset is more accurate than random chance, the meta-learner can still converge to a
 859 highly effective noise-correction policy. This finding enhances the practical applicability of MSPO,
 860 as it suggests that a nearly-clean, rather than perfectly-clean, meta-dataset is often sufficient.

864
865
866
867
868
869
870
871
872
873
Table 7: Sensitivity of MSPO to noise within the meta-dataset D_{meta} . Experiments were run on
Golden HH with 30% main training set noise (Llama-2-7B).

Noise Ratio in D_{meta}	MSPO Final Win Rate (%)
0% (Clean)	96.3 ± 0.4
5%	95.8 ± 0.5
10%	95.1 ± 0.6
15%	94.2 ± 0.8

874
875
876
877
Sensitivity to Meta-Dataset Size. To guide practitioners on the practical application of
MSPO, we investigate its sensitivity to the size of the clean meta-dataset, $|D_{meta}|$. Using
the same setup as before (Golden HH, 30% training noise), we varied the number of sam-
ples in D_{meta} from a very small set of 50 up to 200. The results are shown in Figure 5.

878
879
880
881
882
883
884
885
886
887
888
889
890
891
The performance of MSPO improves as the size of the
meta-dataset increases, which is expected as a larger
meta-set provides a more stable and accurate gradi-
ent for the meta-learner. However, the curve demon-
strates diminishing returns. A significant performance
jump is observed when moving from 50 to 100 samples.
Beyond 150 samples, the performance gains become
marginal. This is a highly encouraging result, as it indi-
cates that MSPO can learn an effective noise-correction
policy from a remarkably small amount of clean data
(approx. 100-150 examples), making it data-efficient
and practical for real-world applications where obtain-
ing large amounts of trusted preference data is expen-
sive.



892
893
894
895
896
897
898
899
900
Figure 5: MSPO’s performance as a func-
tion of the meta-dataset size ($|D_{meta}|$).

Table 8: A qualitative example of MSPO successfully correcting a noisy preference label.

Item	Content
Prompt	How can I stop procrastinating and be more productive?
Response A (Nominally Preferred, y_w)	You just need to have more discipline. Try to focus harder and avoid distractions. Make a to-do list and stick to it no matter what. It's all about willpower.
Response B (Nominally Dispreferred, y_l)	Several techniques can help. You could try the Pomodoro Technique... breaking down large tasks... Prioritizing tasks using an Eisenhower Matrix...
Original Label PPLDiff (A, B; $\pi_{\theta^{(t)}}$)	Response A \succ Response B (Noisy Label) +3.14 (Model finds B more plausible)
MSPO Label (\hat{p}_ϕ)	0.07 (Effectively reverses preference, strongly favoring B)

901
902
903
904
905
906
907
908
909
910
911
912
Table 9: A qualitative example of an MSPO failure case, where a misleading PPLDiff signal leads
to an incorrect correction.

Item	Content
Prompt	What is the primary cause of the aurora borealis?
Response A (Nominally Preferred, y_w)	It is caused by moonlight refracting off of ice crystals in the upper atmosphere, similar to a rainbow.
Response B (Nominally Dispreferred, y_l)	The breathtaking phenomenon of the aurora is a direct result of lunar gravity interacting with the Earth’s magnetic poles, creating shimmering curtains of light.
Original Label PPLDiff (A, B; $\pi_{\theta^{(t)}}$)	Response A \succ Response B (Slightly less incorrect) +1.82 (Model finds the more fluent, but wrong, Response B more plausible)
MSPO Label (\hat{p}_ϕ)	0.15 (Incorrectly reinforces the model’s bias by favoring B)

913
914
915
916
917
Qualitative Case Study. To provide a more intuitive understanding of MSPO’s mechanism, we
present a representative case study from the Golden HH dataset (trained with 30% random flip noise)
in Table 8. This example showcases how MSPO performs instance-level error correction. In this
case, the original noisy label favors a generic and unhelpful response. The partially-aligned main
LLM correctly identifies the higher quality of the alternative response, resulting in a large positive
PPLDiff. MSPO’s meta-learner successfully interprets this conflict and generates a corrective soft

918 label close to 0, effectively reversing the noisy preference and guiding the LLM to learn from the
919 more helpful response.
920

921 Conversely, Table 9 presents a failure case. Here, both responses are factually incorrect, but Re-
922 sponse B is more fluent and structured. The main LLM, biased towards fluency, incorrectly assigns
923 a higher likelihood to Response B, resulting in a positive PPLDiff. The original label (correctly)
924 preferred the slightly less wrong Response A. MSPO’s meta-learner, trusting the misleading PPLD-
925 iff signal, incorrectly generates a low soft label, reinforcing the model’s bias towards fluency over
926 factuality. This highlights a limitation: MSPO’s effectiveness is tied to the quality of the PPLDiff
927 signal, which may not always correlate with nuanced aspects of preference like factual accuracy.
928
929
930
931
932
933
934
935
936
937
938
939
940
941
942
943
944
945
946
947
948
949
950
951
952
953
954
955
956
957
958
959
960
961
962
963
964
965
966
967
968
969
970
971